Biomimetic Models of the Photosynthetic Reaction Center Based on Ruthenium−Polypyridine Complexes

Marlene Kropf, Dietmar van Loyen, Oliver Schwarz, and Heinz Dürr*

Universität des Saarlandes, FB 11.2 Organic Chemistry, D-66041 Saarbrücken, Germany

Received: November 3, 1997; In Final Form: January 27, 1998

Mimicking the fundamental processes of the photosynthetic reaction center is a large field of research over the past decade. We present as biomimetic model systems for electron transfer the mono- and heteroleptic ruthenium complexes **2**−**9** containing differently substituted bipyridazine−glycol ligands. Depending on the number of glycol chains of the complexes **2**−**9**, they are divided into three classes: **A** (2 branches, **2**−**4**); **B** (3 branches, **5**−**6**) and **C** (6 branches, **7**−**9**). UV, fluorescence, single-photon counting, and laser flash photolysis were employed as techniques for photophysical characterization. Redox properties were determined using cyclic voltammetry. Detailed steady-state quenching studies of **2**−**9** with MV^{2+}, OV^{2+}, and MPVS have shown different supramolecular interactions between sensitizer and acceptor in the case of MV^{2+}. These effects may be explained by $\pi-\pi$ donor−acceptor attractions as well as hydrophobic interactions. Supporting molecular modeling studies have been done. The suitability as biomimetic model systems was shown by testing the ruthenium complexes **2**−**9** in artificial photosynthesis systems. Two typical reactions were selected: the sacrificial reduction of water and the reduction of CO_2 to CH_4. The use of **2**−**9** leads to satisfactory hydrogen production from the reduction of water. In the CH_4/CO_2 system, complexes **7**−**9** worked efficiently.

Introduction

The elucidation of the structural unit of the photochemical reaction center by Huber, Michel, and Deisenhofer was a breakthrough in the fields of organic chemistry and biochemistry.[1−3] Numerous kinetic studies followed to characterize the detailed photochemical and thermal steps involved in the intrinsic electron transfer of the natural system.[4−7] To study and clarify in more detail the photochemical primary steps in the photochemical reaction center, model compounds were investigated. Basically two approaches for models of the artificial photosynthetic units can be envisaged: (1) covalently linked subunits based on donor−sensitizer−acceptor triads or polyads or (2) noncovalently linked supramolecular structures containing the same entities however in separate molecules that allow for host−guest interaction.

The second approach is in principle more close to nature since in the natural system the components are not directly linked but rather held together by a supramolecular structure involving the protein matrix.[8,9] Nevertheless this topic has been investigated to a limited extent.[10−16] The covalently linked systems **1** studied by various researchers are in principle linear systems of the type **1a**.[17−21] Nature's system however consists of two branches, so the system **1b** we have published as a model structure comes more close to the natural system (Scheme 1).[22,23]

In this paper we present basic model studies of the electron-transfer process of Ru−polypyridine complexes **A:2**−**4**, **B:5**−**6**, and **C:7**−**9** (Scheme 2), being able to establish noncovalently interacting supramolecular assemblies with suitable quenchers such as mono- or bisviologens. **A:2**−**4** consist of symmetrical structures of the type sensitizer−spacer−acceptor and have been designed as biomimetic model systems which are comparable to nature's subunits (M- and L-branch). It is however likely that in contrast to the photosynthetic reaction center both branches are involved in the electron-transfer process. Additionally we describe nonnatural systems of the type **B:5**−**6** (three branches) and **C:7**−**9** (six branches), which allow for multiple bonding, in principle.

SCHEME 1: Schematic Drawing of Covalently Linked Model Compounds for the Photochemical Reaction Center: Unidirectional, 1a, and Our Bidirectional System, 1b

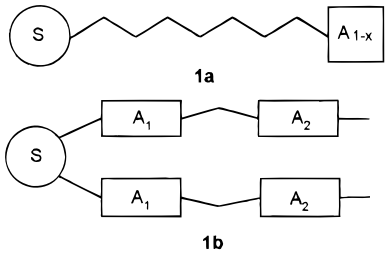

Steady-state quenching experiments and molecular modeling studies show that supramolecular self-organizing sensitzer−acceptor assemblies occur. Absorbed light energy induces via a charge-separated state classical redox chemistry such as water and CO_2 reduction to give hydrogen or methane, respectively.

Experimental Section

The synthesis of the complexes bis(6,6′-dimethyoxy-3,3′-bipyridazine)(6,6′-bis[8-hydroxy-3,6-dioxaoctyl-1-oxy]-3,3′-bipyridazine)ruthenium(II) dichloride (**2a**), bis(6,6′-dimethyoxy-3,3′-bipyridazine)(6,6′-bis[11-hydroxy-3,6,9-trioxaundecyl-1-oxy]-3,3′-bipyridazine)ruthenium(II) dichloride (**2b**), bis(6,6′-dimethyoxy-3,3′-bipyridazine)(6,6′-bis[8-((4-methoxyphenyl)oxy)-3,6-dioxaoctyl-1-oxy]-3,3′-bipyridazine)ruthenium(II) dichloride (**3**), bis(6,6′-dimethyoxy-3,3′-bipyridazine)(6,6′-bis[5-benzyloxy-3-oxapentan-1-oxy]-3,3′-bipyridazine)ruthenium(II) dichloride

S1089-5639(98)00062-0 CCC: $15.00
Published on Web 03/26/1998

SCHEME 2: Chemical Structures and Schematic Drawings of the Biomimetic Ruthenium−Polypyridine Complexes A:2−4 (Two Branches), B:5−6 (Three Branches), and C:7−9 (Six Branches)

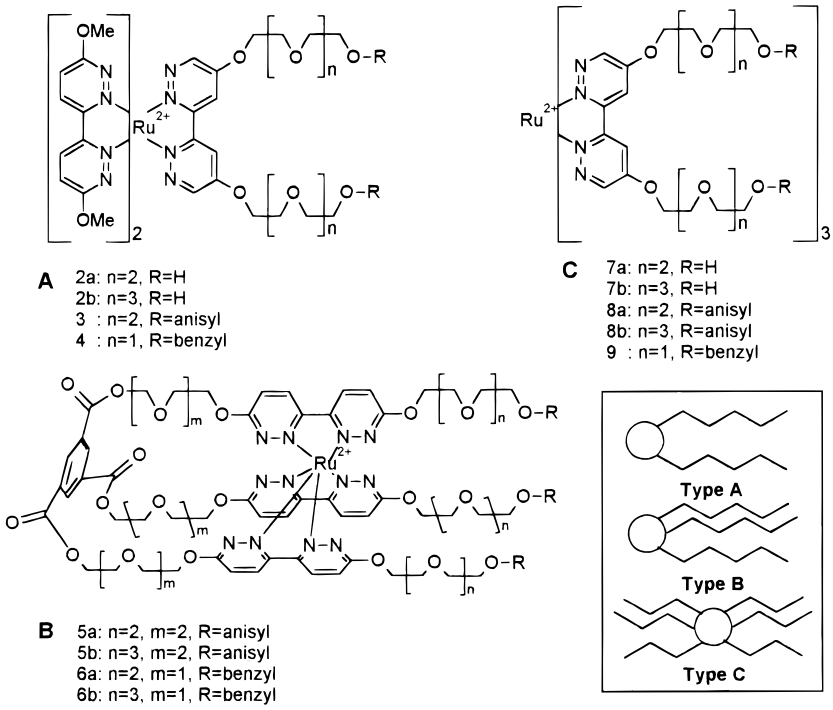

(**4**), tris(6-(8-hydroxy-3,6-dioxaoctyl-1-oxy)-6′-[8-((4-methoxyphenyl)oxy)-3,6-dioxaoctyl-1-oxy]-3,3′-bipyridazine)-1,3,5-benzenetricarboxylate-ruthenium(II) dichloride (**5a**), tris(6-(11-hydroxy-3,6,9-trioxaundecyl-1-oxy)-6′-[8-((4-methoxyphenyl)oxy)-3,6-dioxaoctyl-1-oxy]-3,3′-bipyridazine)-1,3,5-benzenetricarboxylate-ruthenium(II) dichloride **5b**, tris(6-(8-hydroxy-3,6-dioxaoctyl-1-oxy)-6′-[8-hydroxy-3,6-dioxaoctyl-1-oxy]-3,3′-bipyridazine)-1,3,5-benzenetricarboxylate-ruthenium(II) dichloride (**6a**), tris(6-(11-hydroxy-3,6,9-trioxaundecyl-1-oxy)-6′-[8-hydroxy)-3,6-dioxaoctyl-1-oxy]-3,3′-bipyridazine)-1,3,5-benzenetricarboxylate-ruthenium(II) dichloride (**6b**), tris(6,6′-bis[8-hydroxy-3,6-dioxaoctyl-1-oxy]-3,3′-bipyridazine)-ruthenium(II) dichloride (**7a**), tris(6,6′-bis[11-hydroxy-3,6,9-trioxaundecyl-1-oxy]-3,3′-bipyridazine)ruthenium(II) dichloride (**7b**), tris(6,6′-bis[8-((4-methoxyphenyl)oxy)-3,6-dioxa-octyl-1-oxy]-3,3′-bipyridazine)ruthenium(II) dichloride (**8a**), tris(6,6′-bis[11-((4-methoxyphenyl)oxy)-3,6-dioxaundecyl-1-oxy]-3,3′-bipyridazine)ruthenium(II) dichloride (**8b**), and tris(6,6′-bis[8-benzyloxy-3-oxapentyl-1-oxy]-3,3′-bipyridazine)ruthenium(II) dichloride (**9**) has been described elsewere.[15] *N*,*N*′-bis(3-sulfonatopropyl)-3,3′-dimethyl-4,4′-bipyridine (MPVS) was prepared according to the literature.[24] Synthesis of the microheterogeneous Pt catalyst and the quasihomogeneous Ru catalyst was performed according to the original procedure by Turkevich (citrate method).[25,26]

N,*N*′-Dimethyl-4,4′-bipyridine (MV^{2+}), *N*,*N*′-dioctyl-4,4′-bipyridine (OV^{2+}), triethanolamine (TEOA), EDTA (disodium salt), sodium bicarbonate, sodium citrate, K_2PtCl_6, $RuCl_3 \cdot 3H_2O$, and $(Bu)_4NBF_4$ were purchased from Aldrich and used without further purification; only TEOA was freshly distilled. Amberlite MB 3 was obtained from Serva. TiO_2−P25 was a gift from Degussa, Darmstadt. Doubly distilled water was used for all reactions.

UV/vis absorption spectra were recorded on a Uvikon 860 (Kontron). Fluorescence spectra and steady-state luminescence were taken using a Hitachi F-3000 spectrometer in degassed aqueous solutions.

In a typical quenching experiment the concentration of the sensitizer was 3.0×10^{-5} mol L^{-1}. Luminescence quantum yields ϕ_L were determined using $Ru(bpy)_3^{2+}$ as standard ($\phi_L = 0.042$).[27,28]

The luminescence lifetimes τ_L were measured in degassed aqueous solutions either with a FL-900 single-photon counter (Edinburgh Instruments) or by laser flash photolysis.[15]

Cyclic voltammetry was performed with a VA Scanner E 612 and Polarecord 626 (Metrohm) coupled to a X,Y-plotter (Rikadenki). The working electrode and the counter electrode were platinum. The reference electrode was a Ag/AgCl (3 M KCl, double junction). $Ru(bpy)_3(PF_6)_2$ was used as a standard.[29] All measurements were recorded in CH_3CN solutions containing 0.1 mol L^{-1} $(Bu)_4NBF_4$ as supporting electrolyte. Typically a scan rate of 100 mV/s was employed. All potentials are given in H_2O versus NHE.

The irradiation experiments were carried out in a 3.5 mL glass cuvette; all samples were degassed with Ar. The light source was a XBO 450 W xenon lamp (Osram) with a cutoff filter KV-418 ($\lambda < 418$ nm) and a 10 cm water cell ($\lambda > 730$ nm) as IR filter. Molecular hydrogen was detected by gas chromatography with a 90-P-WLD instrument (Varian) (column 2 m, 1/8 in., molecular sieve 0.5 nm, carrier gas N_2) and methane with a GC-14 A (FID-Detector) linked to an integrator Chromatopac C-R6A (Shimadzu) (column: Haye-Sep D, 10 ft × 1/8 in., 100/120 mesh (Macherey Nagel), carrier gas N_2).

The photolysis experiments were run with the following concentrations: (a) reduction of water,: 4.0×10^{-5} mol L^{-1} sensitizer, 5.0×10^{-4} mol L^{-1} MV^{2+}, 1.0×10^{-3} mol L^{-1} EDTA, 4.0×10^{-5} mol L^{-1} Pt catalyst, 5.0×10^{-2} mol L^{-1} phosphate buffer (pH 7); (b) reduction of CO_2, 1.4×10^{-4} mol L^{-1} sensitizer, 7.0×10^{-3} mol L^{-1} MPVS, 1.0×10^{-1} mol L^{-1} TEOA, 5.0×10^{-2} mol L^{-1} $NaHCO_3$, 2.0×10^{-4} mol L^{-1} Ru catalyst. The pH of the solution was adjusted to 7.8 with CO_2.

All molecular modeling calculations were performed with the

TABLE 1: Absorption Properties of the Complexes 2−9 in H_2O

		λ_{max}abs (nm) (ϵ (10^4 M^{-1} cm^{-1}))					
cpx		1.MLCT	2.MLCT	3.MLCT	1.LC	2.LC	3.LC
A	**2a**	451 (4.08)	412 (4.11)	343 (4.06)	287 (4.56)	258 (4.55)	221 (4.75)
	2b	450 (4.02)	412 (4.03)	341 (4.03)	288 (4.49)	257 (4.51)	220 (4.69)
	3	456 (4.10)	412 (4.12)	346 (4.15)	289 (4.62)	257 (4.65)	220 (4.89)
	4	458 (4.05)	414 (4.09)	340 (4.05)	288 (4.52)	258 (4.52)	
B	**5a**	456 (4.23)	414 (4.25)	349 (4.18)	290 (4.68)	258 (4.65)	218 (5.03)
	5b	454 (4.21)	414 (4.24)	344 (4.00)	292 (4.67)	260 (4.62)	222 (4.94)
	6a	456 (4.21)	414 (4.24)	346 (4.14)	292 (4.61)	258 (4.62)	222 (4.82)
	6b	455 (4.21)	416 (4.26)	344 (4.14)	293 (4.67)	258 (4.66)	218 (5.00)
C	**7a**	451 (4.21)	414 (4.23)	344 (4.15)	290 (4.61)	260 (4.63)	224 (4.79)
	7b	451 (4.20)	411 (4.18)	356 (4.12)	294 (4.55)	258 (4.57)	223 (4.77)
	8a	458 (4.24)	416 (4.29)	343 (4.19)	287 (4.77)	265 (4.68)	226 (4.88)
	8b	457 (4.23)	415 (4.26)	343 (4.16)	287 (4.76)	262 (4.66)	221 (5.03)
	9	461 (4.24)	417 (4.29)	347 (4.18)	292 (4.69)	261 (4.68)	226 (4.99)

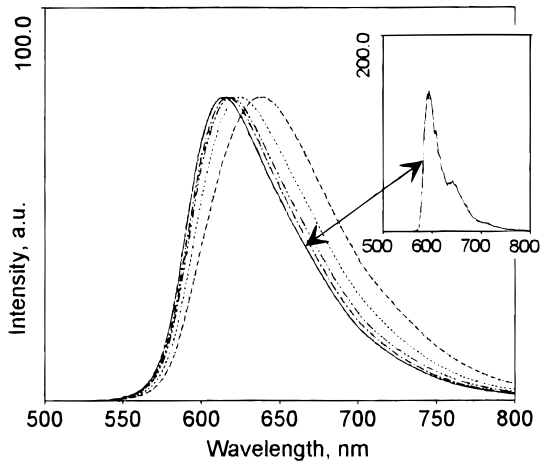

Figure 1. Luminescence spectra of **7a** (···), **7b** (- - -), **8a** (−·−), **8b** (−··−), and **9** (—) (c(cpx) = 10^{-5} mol L^{-1}) at 298 K (inset: **9** at 77 K).

MM+ force field (HyperChem 5.0, Hypercube, Inc.) using the conjugate gradient method Polak-Ribiere with a rms gradient of 10^{-3}.

Results and Discussion

The UV spectra for all Ruthenium coordination compounds **2**−**9** are typical and show absorptions in the range 450−461 nm for the first MLCT transition. The spectra possess rather similar absorption for all three MLCT bands; thus one can conclude that the ligand field in **2**−**9** is very similar (Table 1).[30]

Fluorescence spectra of the Ru−bipyridazine complexes **2**−**9** give rise to considerable Stokes shifts of 154−184 nm. Whereas the fluorescence band is unstructured at room temperature, a splitting into two bands is observed at low temperature (77 K) (Figure 1). Analogous to Ru−bipyridine complexes, the fluorescence at lower wavelengths can be assigned to the emission from a ^{3}MLCT state; the band at higher wavelengths may belong to a ^{3}MC.[31] Furthermore the energy of the 0−0 transition (E_{0-0}) is available from the low-temperature excitation and emission spectra (Table 2).

Lifetime measurements with **2**−**9** were carried out with a LASER equipment or a single-photon counter. Lifetimes τ_L determined by this procedure are collected in Table 3.

The lifetimes of **2**−**9** are larger by a factor of 2−6 compared to $Ru(bpy)_3^{2+}$. This fact can also be observed on $Ru(bpdz)_3^{2+}$ (τ_L = 1.189 μs)[32] and may be due to the possible stabilization of the excited state by the SLUMO in bipyridazine systems.[33]

Larger spacer groups as in **2a**,**b** and **7a**,**b** also increase the lifetimes of the Ru complexes, as observed previously by R. Schwarz and M. Seiler.[34,35] This effect however is restricted to −OH end groups in **2** and **7**. The increasing polarity due to the larger glycol spacer chains in **5b**, **6b**, or **8b** may reduce the lifetimes however slightly compared to **5a**, **6a**, and **8a**.

TABLE 2: Luminescence Properties of the Complexes 2−9

		λ_{max} em (nm)		Φ_L (%)	E_{0-0} (kJ/mol)
cpx		at 298 K[a]	at 77 K[b]	at 298 K[a]	at 77 K[b]
A	**2a**	624	599, 642	3.5	206.9
	2b	627	599	3.3	207.0
	3	634	592, 645	4.0	206.5
	4	617	589, 641	4.7	207.6
B	**5a**	618	587, 640	5.0	207.5
	5b	622	603	4.8	206.3
	6a	620	599, 640	5.3	206.7
	6b	625	594	4.8	206.2
C	**7a**	624	600	3.0	205.8
	7b	637	601	2.4	205.2
	8a	616	588, 643	5.4	207.4
	8b	617	589, 640	5.0	207.5
	9	613	595, 642	6.5	208.2

[a] c(cpx) = 10^{-5} mol L^{-1} in H_2O. [b] c(cpx) = 10^{-6} mol L^{-1} in EtOH.

TABLE 3: Luminescence Lifetimes and Constants for the Radiative (k_r) and Nonradiative (k_{nr}) Reaction in H_2O at 298K (c(cpx) = 4 × 10^{-5} mol L^{-1})

	cpx	τ_L (μs)	k_r (10^5 s^{-1})	k_{nr} (10^5 s^{-1})
A	**2a**	1.928	0.182	5.005
	2b	2.056	0.161	4.703
	3	2.434	0.164	3.944
	4	2.836	0.166	3.360
B	**5a**	2.478	0.202	4.036
	5b	2.318	0.207	4.107
	6a	2.606	0.203	3.634
	6b	2.439	0.197	3.903
C	**7a**	1.878	0.160	5.165
	7b	1.943	0.124	5.023
	8a	2.491	0.217	3.797
	8b	2.406	0.278	4.156
	9	3.459	0.188	2.891

Quenching Experiments and Electron Transfer. Quenching experiments for the sensitizers (S) **2**−**9** were carried out with various acceptors (A): MV^{2+} ($E°$ = −0.41 V), OV^{2+} ($E°$ = −0.45 V), and MPVS ($E°$ = −0.79 V). All values of the quenching constants k_q observed for **2**−**9** are smaller than the values for $Ru(bpy)_3^{2+}$ (Table 4). This is most probably caused by steric effects. The more bulky ligands of the sensitizers allow only a weaker interaction of the sensitizer with a quencher (variable distance model).[36] This explains also the slightly higher values of quenching constants for the biomimetic heteroleptic Ru complexes **A:2**−**4** since the smaller number of bulky glycol groups favors steric interaction in the encounter

TABLE 4: Electrochemical Properties and Quenching Constants

	cpx	$E_{Ru}^{2+/3+}$ [a]	$E_{Ru}^{2+*/3+}$ [a]	$E_{Ru}^{2+/+}$ [a]	$E_{Ru}^{2+*/+}$ [a]	k_q (10^7 L mol^{-1} s^{-1}) in H_2O		
						MV^{2+}	OV^{2+}	MPVS
A	**2a**	1.42	−0.72	−1.11	1.03	1.10	3.11	
	2b	1.45	−0.70	−1.10	1.05	1.44	2.85	
	3	1.37	−0.77	−1.15	0.99	2.38	3.61	
	4	1.35	−0.80	−1.15	1.00	1.70	3.46	
B	**5a**	1.33	−0.82	−1.25	0.90	2.01		
	5b	1.36	−0.78	−1.21	0.93	1.45		
	6a	1.36	−0.78	−1.21	0.93	0.57		
	6b	1.35	−0.79	−1.22	0.91	0.49		
C	**7a**	1.42	−0.71	−1.15	0.98	1.29	1.78	
	7b	1.33	−0.82	−1.25	0.90	1.21	2.60	0.96
	8a	1.32	−0.83	−1.26	0.89	1.88	6.24	
	8b	1.48	−0.65	−1.08	1.05	1.81	4.69	1.15
	9	1.35	−0.81	−1.23	0.93	1.08	1.95	1.06

[a] V vs NHE.

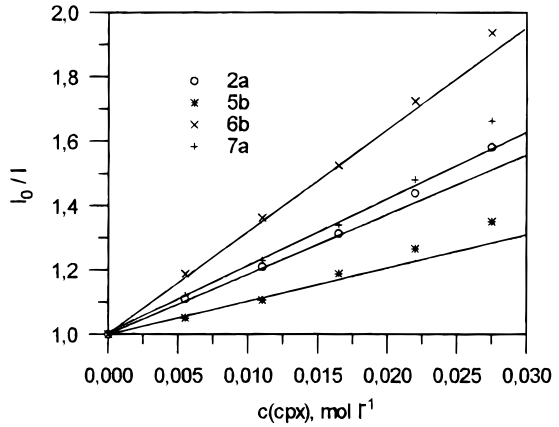

Figure 2. Stern−Volmer plot of **2a** (+), **5b** (*), **6b** (×), and **7a** (○) with MV^{2+} in H_2O (c(cpx) = 2 × 10^{-5} mol L^{-1}).

cage complex of **2**−**4** and MV^{2+}. The larger k_q values for anisyl-substituted complexes **A:3**, **B:5**, and **C:8** result probably from higher diffusion coefficients for these molecules due to lack of free OH groups (as in unsubstituted glycol chains) to form hydrogen bonds to solvent molecules. An additional donor−acceptor $\pi-\pi$ interaction may lead to a stacking of the phenyl rings in **3**−**6** and **8**, **9**, and the quencher MV^{2+}, which also favors the formation of the encounter cage complex. As for the quenching with the cyclic bisviologen cyclo(bis-(1,1′-xylylene-4,4′-bipyridinium) ($E°$ = −0.47 V), this interaction is most distinct with anisyl-substituted glycol chains.[15] Nevertheless all Stern−Volmer plots of the Ru complexes **2**−**9** quenched with MV^{2+} are slightly nonlinear at higher concentrations (S:A > 1:500) (Figure 2). Although this effect is less obvious than with the cyclic bisviologen cyclo(bis(1,1′-xylylene-4,4′-bipyridinium), it is a hint for supramolecular effects between the acceptor MV^{2+} and the sensitizer so that at higher quencher concentration static and dynamic quenching are superposed.

The assumptions made above are supported by molecular modeling results. For all molecules **A**−**C** having benzyl or anisyl groups at the end of the polyglycol chain, geometry optimization results in the formation of a $\pi-\pi$ complex between the MV^{2+} (quencher) and the aromatic systems at the branch terminus. In principle there may be more than one binding site for the quencher. As an example Figure 3 shows the space-filling model of the anisyl-substituted type **C** system **8a** with one molecule of MV^{2+} embedded in the side chains. We assume that Coulombic interactions between the Ru^{2+} center of **8a** and the positive charges in MV^{2+} are provoking a rather streched geometry of the assembly **8a**/MV^{2+}. Additionally arene−arene interactions in **8a** stabilize a flat geometry as well.

The biomimetic model complexes with unsubstituted glycol chains of type **A 2a,b** and **4** as well as those of type **C 7b** and **9** show an additional nonlinearity in their Stern−Volmer plots at lower concentration of MV^{2+}. This is most pronounced with the type **A** complex **4** (Figure 4). The fact that two different excited states are involved is not very likely.[37] We suggest that at initial almost stoichiometrical concentrations (S:A < 1:10) the quencher is attached to the ethylene glycol chains of the sensitizers. Such a binding with poly(ethylene glycol) subunits in porphyrins has been established by Gunther and Johnston.[38,39] This host−guest interaction is thought to favor static quenching at lower concentrations, so the slope of the Stern−Volmer plot is steeper at the beginning.

The assumption of host−guest interactions is supported by a quenching study using the sterically more encumbered and more hydrophobic OV^{2+}. Here the Stern−Volmer plots are linear, indicating that the long alkyl chains decrease or eliminate host−guest aggregates. The same result has been found for the Stern−Volmer plots in quenching experiments with the complexes **7b**, **8a**, and **9** and MPVS, which is also sterically more demanding than MV^{2+}.

The results of the steady-state quenching study with the complexes **2**−**9** and MV^{2+} are combined in Figure 5 using a Rehm−Weller plot. The positions of all observed k_q values are lower compared to the theoretical Rehm−Weller curve.[40,41] This also seems to imply supramolecular aggregates.

Photosensitized Reduction of Water and CO_2. The ability to use the electron transfer of the Ru complexes **2**−**9** for artificial photosynthesis should show that the charge-separated state may be used in a chemical process. This renders **2**−**9** to be real model systems with properties comparable with those found in nature. A study of this type is rather rare in the literature.

Here we present such an application for two artificial photosynthetic systems: (1) the sacrificial water reduction (reaction 1) and (2) the sacrificial reduction of carbon dioxide to methane (reaction 2).

$$2H^+ + 2e^- \rightarrow H_2 \qquad E° = -041\ \text{V} \quad (1)$$

$$CO_2 + 8H^+ + 8e^- \rightarrow CH_4 + 2H_2O \qquad E° = -0.24\ \text{V} \quad (2)$$

In both systems absorbed light energy is transferred from a photoexcited sensitizer via an acceptor (electron relay) on the substrate (water protons or carbon dioxide) (vide infra).

A large number of sensitizers have been investigated in Graetzel's and our group in the water cleavage system (reaction

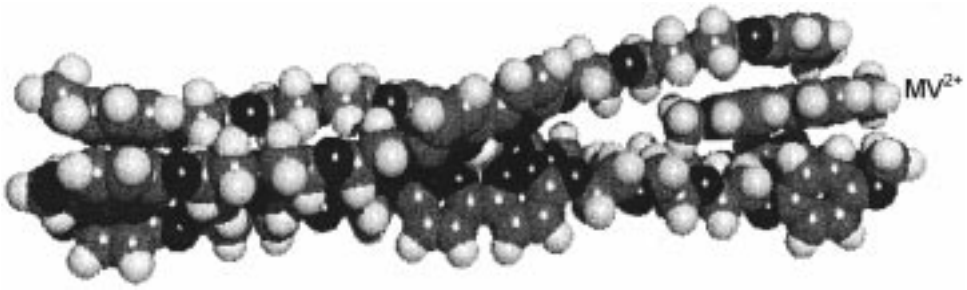

Figure 3. MM+ minimized structure of **8a** with one molecule MV^{2+} embedded between the poly(ethylene glycol) chains.

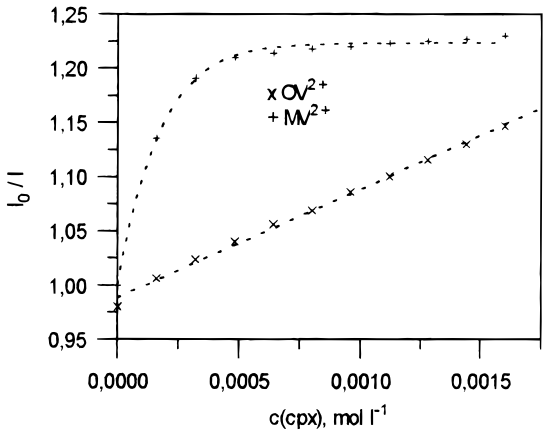

Figure 4. Stern−Volmer plot for **4** with MV^{2+} (+) and OV^{2+} (×) in H_2O (c(cpx) = 2×10^{-5} mol L^{-1}).

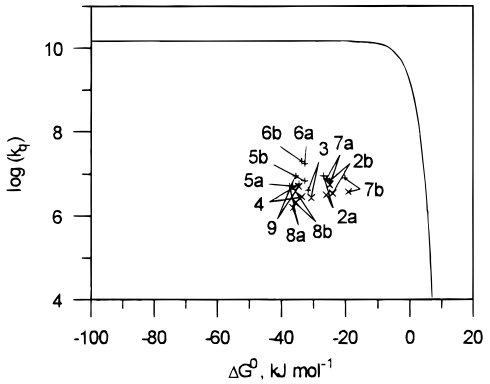

Figure 5. Rehm−Weller plot: values calculated for **2**−**9** with MV^{2+} (+) and **2**−**4**, **7**−**9** with OV^{2+} (×) in H_2O (c(cpx) = 3×10^{-5} mol L^{-1}). ΔG values calculated from the Rehm−Weller equation $\Delta G = F[E(S^*/S^+) - E(A/A^-)]$; F = Faraday constant. (−, theoretical Rehm−Weller plot).[40,41]

1), especially metal complexes such as ruthenium−tris(polypyridines) and −bis(diazines).[42−47] Because of the structural relationship to the sensitizer of the natural photosynthesis, chlorophyll, many members of the class of porphines have been studied, too.[48−51] The application in the standard sacrificial water reduction system however is limited mostly because of decreased photostability of the porphyrins and the tendency of aggregation as well as poor solubility of the mostly hydrophobic phthalocyanines and porphyrazines especially in aqueous solutions.

In the case of the CO_2/CH_4 system (reaction 2) only few studies all investigating ruthenium−polypyridines as sensitizers have been carried out.[24,52,53] A reason may be the kinetic barrier for the reaction, where the reduction of CO_2 to CH_4 requires the accumulation of eight electrons on the catalyst. Nevertheless, the use of supramolecular covalently linked sensitizer−acceptor systems should increase the efficiency of the system compared to the use of an external electron relay (acceptor).[54,55]

SCHEME 3: Oxidative Pathway of a Photoinduced Redox Reaction in a Four-Component System (See Text). S: Sensitizer, A: Electron Acceptor (Relay), D: Electron Donor, cat.: Catalyst

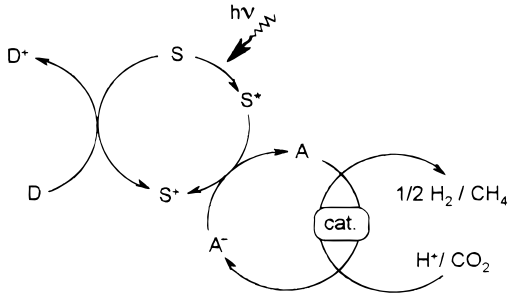

In both reactions 1 and 2 the quenching of the excited state of the sensitizer is possible via an oxidative or reductive pathway, depending on the redox potential of the photoexcited state. This fact results in two possible reaction mechanisms. In the current study all reactions—according to the potentials determined—should proceed via the oxidative mechanism (Scheme 3).

The photoexcited sensitizer **S*** transfers an electron to the electron relay **A** (MV^{2+} or MPVS) and is thermally regenerated by an electron donor **D** (EDTA or TEOA), which is irreversibly oxidized by electron transfer to $MV^{\bullet+}$ (=A^-).[31,56] Thus we operate with a sacrificial system. The catalyst (cat.) determines which reduction process occurs to afford molecular hydrogen or methane or both.

For the water reduction with **2**−**9** the relay MV^{2+} and the donor EDTA were employed. As catalyst a microheterogenic TiO_2(P25)−Pt antenna catalyst (platinium clusters linked to the surface of TiO_2) was used.[46] In the CO_2 reduction the relay MPVS and the donor TEOA were selected. Here a quasihomogeneous Ru−sol was taken as a catalyst.

Since the efficiency of the sacrificial systems described above strongly depends on the reaction conditions, especially on the quality of the catalyst, $Ru(bpy)_3^{2+}$ served as a standard. To allow comparison of the various yields of reaction products, rather simple and reproducible reaction conditions were chosen.

The amounts of hydrogen or methane, respectively, detected after the first hour of continuous photolysis are given in Figure 6. These results will be discussed in the following sections.

Water Reduction by Visible Light. According to the amounts of hydrogen produced, the sensitizers can be divided into three groups following the classification pattern for the biomimetic model systems. The sensitizers of type **A:2**−**4** (two branches) develop only hydrogen in a poor yield, whereas the type **B** compounds **5**−**6** (three branches) give good results. The most effective complexes, however, are those of type **C:7**−**9**

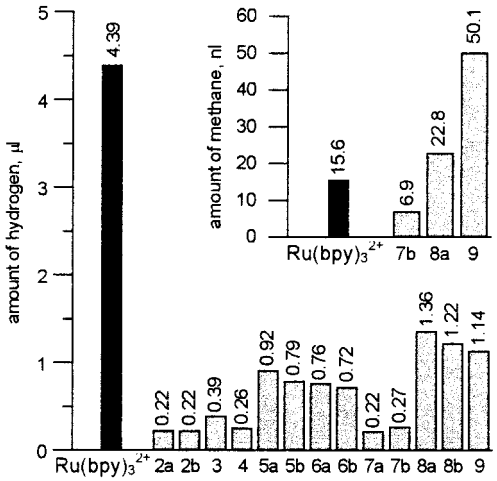

Figure 6. Hydrogen evolution after 60 min of continuous photolysis (c(sensitizer) = 4×10^{-5} mol L^{-1}; c(relay) = 5×10^{-4} mol L^{-1}; c(donor) = 10^{-3} mol L^{-1}; c(catalyst) = 4×10^{-5} mol L^{-1}). Inset: Methane evolution after 60 min of continuous photolysis (c(sensitizer) = 1.4×10^{-5} mol L^{-1}; c(relay) = 7×10^{-3} mol L^{-1}; c(donor) = 10^{-1} mol L^{-1}; c(catalyst) = 2.0×10^{-4} mol L^{-1}).

(six branches) with the exception of **7a,b**, which are as inefficient as **2**−**4**. The much smaller constants k_r for the radiative reaction (Table 3) in the case of **7a,b** imply that a smaller part of the light energy absorbed during the photoexcitation is converted to luminescence energy than for **8** and **9**. The preferred thermal deactivation may be a reason for poor efficiency.

According to the good quenching results with MV^{2+}, much higher amounts of hydrogen are to be expected for the sensitizers **2**−**4**. However the relatively inefficient radiative reaction and the small reaction enthalpy because of the more positive redox potentials of the excited complex seem to limit the efficiency of these complexes.

A comparison between the three classes of systems **A**, **B**, and **C** shows that the anisyl-substituted complexes **A:3**, **B:5**, and **C:8** are always superior to the others, which is in agreement with the quenching studies (vide supra).

Nevertheless all Ru−bipyridazine complexes **2**−**9** produce 3−20 times less hydrogen compared with the standard Ru(bpy)$_3^{2+}$. This fact may be due to a smaller reaction enthalpy in contrast to the standard in some cases. On the other hand, the formation of the encounter cage complex is likely to be more complicated because of the bulky ligands of the complexes **2**−**9**. Finally the relay that has to transfer the electron from the sensitizer on the catalyst may work less efficiently due to supramolecular interactions of MV^{2+} and the oligo(ethylene glycol) substituents of the sensitizers. Thus in the solution the part of the reduced relay available for diffusion is diminished. The latter argument which is in agreement with the results of the steady-state quenching studies and molecular modeling (vide supra) is supported by the fact that using the cyclic bisviologen cyclo(bis-(1,1′-xylylene-4,4′-bipyridinium) as an electron relay no molecular hydrogen could be detected. The explanation may be the supramolecular $\pi-\pi$ interaction of the bisviologen and the sensitizer at higher concentrations and thus a faster back electron transfer.[15] This interaction, even much more enhanced compared to MV^{2+}, seems to exclude the application of the bisviologen as a cyclic electron relay in a diffusionally dependent system like the sacrificial water reduction.

Nevertheless using MV^{2+} as an electron relay all sensitizers **2**−**9** are doing chemistry in the sacrificial system, indicating that here the electron-transfer step can be used in a chemical reaction.

Light-Induced CO_2 Reduction. The most efficient complexes, **7b**, **8a**, and **9**, also have been studied in the sacrificial CO_2 reduction. Here the catalyst has to collect eight electrons from the relay to reduce one molecule of CO_2 to CH_4 (kinetic barrier), which is the thermodynamically favored reaction. The generation of potential side products such as C_2H_6, C_2H_4, and even hydrogen has not been investigated during this study. Because of the increased demands on the catalyst, the amounts of methane are generally smaller than those of hydrogen in the water reduction system.

The amounts of methane detected (after 60 min of photolysis) show that **8a** and especially **9** are more efficient than Ru(bpy)$_3^{2+}$ (Figure 6). Compound **9** produces nearly 3 times more methane than the standard. A comparison with the physical data gives a direct correlation between methane volumes and luminescence lifetimes τ_L or luminescence quantum yields ϕ_L, respectively. The higher the values for τ_L and ϕ_L, the more methane is produced. To the best of our knowledge Ru complex **9** of the compounds of type **C** (six branches) is the most efficient sensitizer in this sacrificial CO_2/CH_4 system with external electron relay to date.

Conclusion

Three classes **A**, **B**, and **C** of different Ru−bipyridazine−poly(ethylene glycol) complexes **2**−**9** have been characterized in their photophysical and electrochemical properties. Steady-state quenching experiments of **2**−**9** with various acceptors such as MV^{2+}, OV^{2+}, and MPVS have been performed. The effects on the quenching process can be summarized as follows: large substituents (steric effects) and hydroxy substitution of the glycol chains (diffusional effects) render the quenching process more difficult; easier accessibility for the acceptor (heteroleptic complexes) and anisyl substitution ($\pi-\pi$ interactions) favor the quenching process. The deviation of the Stern−Volmer plots for **2**−**9**—most clearly with anisyl-substituted glycol chains—to more positive values at higher concentrations of the quencher MV^{2+} may be explained by these $\pi-\pi$ donor−acceptor interactions. In addition the anisyl-free-substituted complexes **2**, **4**, **7**, and **9** show a flattening of the Stern−Volmer plots at lower quencher concentrations. It is likely that this effect is due to interaction of acceptor molecules with the oligo(ethylene glycol) chains. Quenching experiments with OV^{2+} and MPVS as well as molecular modeling studies support the assumptions concerning the supramolecular interaction. The results of the steady-state quenching studies are reflected in the behavior of the Ru complexes **2**−**9** in systems for artificial photosynthesis. The application in the sacrificial water reduction system leads to satifactory results. Hydrogen could be detected in every case, although the efficiency is less than for typical sensitizers such as Ru(bpy)$_3^{2+}$. The best result was obtained for the homoleptic compound **8a**. In the case of CO_2 reduction type **C** complexes **7**−**9** were employed to yield outstanding amounts of methane, especially for **9**, which is the best sensitizer to date for methane generation under these conditions.

The studies presented prove the ruthenium coordination compounds **2**−**9** to be model systems for the photosynthetic reaction center not only because of supramolecular donor−acceptor interactions but also because of the feasibility of using the electron-transfer step in classical chemical reactions storing the absorbed light energy in chemical products such as hydrogen or methane.

Acknowledgment. Financial support from the Volkswagen Stiftung is gratefully acknowledged. We thank Prof. Dr. I. Willner, the Hebrew University of Jerusalem, Jerusalem 91904, Israel, for the time-resolved laser spectroscopy.

References and Notes

(1) Deisenhofer, J.; Michel, H. *Angew. Chem.* **1989**, *101*, 782.
(2) Lancaster, C. R. D.; Michel, H. *Photosynth. Res.* **1996**, *48*, 65.
(3) Huber, R. *Angew. Chem.* **1989**, *101*, 849.
(4) Allen, J. P.; Feher, G.; Yeates, T. O.; Komiya, H.; Rees, D. C. *Proc. Natl. Acad. Sci.* **1988**, *85*, 8847.
(5) Bradforth, S. E.; Jimenez, R.; van Mourik, F.; van Grondelle, R.; Fleming, G. R. *J. Phys. Chem.* **1995**, *99*, 16179.
(6) Joo, T.; Jia, Y.; Yu, J. Y.; Jonas, D. M.; Fleming, G. R. *J. Phys. Chem.* **1996**, *100*, 2399.
(7) Gasyna, Z.; Schatz, P. N. *J. Phys. Chem.* **1996**, *100*, 1445.
(8) Michel Beyerle, M. E.; Plato, M.; Deisenhofer, J.; Michel, H.; Bixon, M.; Jortner, J. *Biochim. Biophys. Acta* **1988**, *932*, 52.
(9) Grunner, M. R. *J. Phys. Chem.* **1996**, *100*, 4277.
(10) Cusack, L.; Nagaraja Rao, S.; Fitzmaurice, D. *Chem. Eur. J.* **1997**, *3*, 202.
(11) Bermann, A.; Izraeli, E. A.; Levanon, H.; Wang, B.; Sessler, J. L. *J. Am. Chem. Soc.* **1995**, *117*, 8252.
(12) Benniston, A. C.; Harriman, A.; Philip, D.; Stoddart, J. F. *J. Am. Chem. Soc.* **1993**, *115*, 5298.
(13) Amabilino, D. B.; Stoddart, J. F. *Chem. Rev.* **1995**, *95*, 2725.
(14) Kropf, M.; Dürr, H.; Collet, C. *Synthesis* **1996**, *5*, 609.
(15) Kropf, M.; Joselevich, E.; Dürr, H.; Willner, I. *J. Am. Chem. Soc.* **1996**, *118*, 655.
(16) David, E.; Born, R.; Kaganer E.; Joselevich, E.; Dürr, H.; Willner, I. *J. Am. Chem. Soc.* **1997**, *119*, 7778.
(17) Gust, D.; Moore, T. A.; Moore, A. L. *Acc. Chem. Res.* **1993**, *26*, 198.
(18) Chen, P.; Meyer, T. J. *Inorg. Chem.* **1996**, *35*, 5520.
(19) Johnson, D. G.; Niemczyk, M. P.; Minsek, D. W.; Wiederrecht, G. P.; Svec, W. A.; Gaines III, G. L.; Wasielewski, M. R. *J. Am. Chem. Soc.* **1993**, *115*, 5692.
(20) Harriman, A.; Odobel, F.; Sauvage, J. P. *J. Am. Chem. Soc.* **1995**, *117*, 9461.
(21) Kurreck, H.; Huber, M. *Angew. Chem., Int. Ed. Engl.* **1995**, *34*, 849.
(22) Seiler, M.; Dürr, H. *Liebigs Ann.* **1995**, 407.
(23) Zahavy, E.; Seiler, M.; Marx-Tibbon, S.; Joselevich, E.; Willner, I.; Dürr, H.; O'Connor, D.; Harriman, A. *Angew. Chem.* **1995**, *107*, 112.
(24) Willner, I.; Maidan, R.; Mandler, D.; Dürr, H.; Dörr, G.; Zengerle, K. *J. Am. Chem. Soc.* **1987**, *109*, 6080.
(25) Turkevich, J. *J. Chem. Phys.* **1945**, *13*, 235.
(26) Turkevich, J.; Stevenson, P.; Hillier, *J. Discuss. Faraday Soc.* **1951**, *11*, 55.
(27) v. Houten, J.; Watts, R. J. *J. Am. Chem. Soc.* **1976**, *98*, 4853.
(28) Caspar, J. V.; Meyer, T. J. *J. Am. Chem. Soc.* **1983**, *105*, 5583.
(29) Belser, P.; von Zelewsky, A. *Helv. Chim. Acta* **1980**, *60*, 1675.
(30) Kitamura, N.; Kawanishi, Y.; Tazuke, S. *Chem. Phys. Lett.* **1983**, *97*, 103.
(31) Juris, A.; Balzani, V.; Barigeletti, F.; Campagna, S.; Belser, P.; von Zelewsky, A. *Coord. Chem. Rev.* **1988**, *84*, 84.
(32) Kropf. M. Thesis, Saarbrücken, 1995.
(33) Ernst, S.; Kaim, W. *Inorg. Chim. Acta* **1986**, *114*, 123.
(34) Seiler, M. Thesis, Saarbrücken, 1994.
(35) Schwarz. R. Thesis, Saarbrücken, 1992.
(36) Rau, H.; Frank, R.; Greiner, G. *J. Phys. Chem.* **1986**, *90*, 2467.
(37) Becker, H. G. O. *Einführung in die Photochemie*, 2nd ed.; Thieme: Stuttgart, 1993; Chapter 7.
(38) Gunther, M. J.; Johnston, M. R. *Tetrahedron Lett.* **1990**, *31*, 4801.
(39) Gunther, M. J.; Johnston, M. R. *Tetrahedron Lett.* **1992**, *33*, 1771.
(40) Rehm, D.; Weller, A. *Ber. Bunsen-Ges. Phys. Chem.* **1969**, *73*, 834.
(41) Rehm, D.; Weller, A. *Isr. J. Chem.* **1970**, *8*, 259.
(42) Kalyanasundaram, K.; Grätzel, M. *Angew. Chem.* **1979**, *91*, 759.
(43) Kalyanasundaram, K.; Kiwi, J.; Grätzel, M. *Helv. Chim. Acta* **1978**, *4*, 547.
(44) Harriman, A.; Porter, G.; Richoux, M. *J. Chem. Soc., Faraday Trans.* **1981**, *77*, 833.
(45) Dürr. H.; Dörr G.; Zengerle, K.; Reis, B.; Braun, A. *Chimia* **1983**, *37*, 245.
(46) Dürr, H.; Bossmann, S.; Beuerlein, A. *J. Photochem. Photobiol. A: Chem.* **1993**, *73*, 233.
(47) Bossmann, S.; Dürr, H.; Mayer, E. *Z. Naturforsch.* **1993**, *48b*, 369.
(48) Harriman, A.; Richoux, M. C. *J. Photochem.* **1980**, *14*, 253.
(49) Adar, E.; Degani, Y.; Goren, Z.; Willner, I. *J. Am. Chem. Soc.* **1986**, *108*, 4696.
(50) Tanno, T.; Wöhrle, D.; Kaneko, M.; Yamada, A. *Ber. Bunsen-Ges. Phys. Chem.* **1980**, *84*, 1032.
(51) Dürr, H.; Hayo, R.; David, E.; Willner, I.; Zahavy, E. *Recl. Trav. Chim. Pays-Bas* **1995**, *114*, 549.
(52) Maidan, R.; Willner, I. *J. Am. Chem. Soc.* **1986**, *108*, 8100.
(53) Dürr, H.; Trierweiler, H. P.; Willner, I.; Maidan, R. *New J. Chem.* **1990**, *14*, 317.
(54) Dürr, H.; Bossmann, S.; Kilburg, H.; Trierweiler, H. P.; Schwarz, R. In *Frontiers in Supramolecular Organic Chemistry and Photochemistry*, 1st ed.; Schneider, H.-J., Dürr. H., Eds.; VCH: Weinheim, 1991; Chapter 20.
(55) Dürr, H.; Bossmann, S.; Schwarz, R.; Kropf, M.; Hayo, R.; Turro, N. J. *J. Photochem. Photobiol. A: Chem.* **1994**, *80*, 341.
(56) Kalyanasundaram, K.; Kiwi, J.; Grätzel, M. *Helv. Chim. Acta* **1978**, *61*, 2720.